Fusion Engineering and Design 188 (2023) 113403

Contents lists available at ScienceDirect

Fusion Engineering and Design

journal homepage: www.elsevier.com/locate/fusengdes

Deuterium retention in CVD diamond: Combined experimental and computational study

J.A. Pittard [a,*], N.A. Fox [a], A. Hollingsworth [b], M.Y. Lavrentiev [b], A. Wohlers [b], Y. Zayachuk [b]

[a] School of Physics, HH Wills Physics Laboratory, University of Bristol, Tyndall Avenue, Bristol, BS8 1TL, United Kingdom
[b] UKAEA, Culham Science Centre, Abingdon, OX14 3DB, United Kingdom

ARTICLE INFO

Keywords:
CVD diamond
Deuterium retention
Thermal desorption spectroscopy
Molecular dynamics

ABSTRACT

Diamond's intrinsic hardness, excellent thermal conductivity and low atomic number make it a highly promising candidate as a plasma facing material. However, as with the previously used graphite, concerns over tritium retention and resultant chemical etching have so far limited research interest in the use of synthetic diamond. In order to study tritium retention, the DELPHI facility at the Culham Centre for Fusion Energy was used to expose polycrystalline diamond samples to a deuterium plasma. Deuterium ions were accelerated to an energy of 0.2 keV to 1 keV for a 5 h exposure time, achieving a fluence of approximately 5.5×10^{21} D m^{-2}. Exposed samples were analysed using Thermal Desorption Spectroscopy. Increasing implantation energy resulted in additional D_2 release peaks observed in the 800–1100 K temperature range that were not seen at lower energies. These peaks were interpreted as an additional bonding mechanism, a likely candidate for which is inter-grain deuterium. Experimental work was complemented with molecular dynamics simulations on the University of Bristol's high performance computer—Blue Crystal Phase 4. In these simulations, both varying implantation energy and the presence of grain boundaries were explored. A two-step etching mechanism was observed, in which the surface initially swelled before carbon removal. No significant differences could be observed on the inclusion of a grain boundary at the energies tested.

1. Introduction

One of most significant problems facing commercial fusion energy is the selection of an appropriate plasma facing material (PFM). The PFM's primary role is to protect more delicate components of the reactor from high thermal loads, high energy neutron flux and low energy ion flux, all whilst exhibiting minimal plasma contamination, damage and fuel retention. It is incredibly challenging to find materials that meet these criteria, and current solutions such as beryllium and tungsten may not be appropriate for planned larger reactors [1–4]. Synthetic diamond grown via chemical vapour deposition (CVD) has potential as a future PFM. Diamond offers many of the benefits of previously used graphite whilst demonstrating reduced chemical etching [5]. Diamond has excellent thermal shock resistance and thermal conductivity, a high cohesive energy and a low atomic number which results in minimal radiative cooling from sputtered ions. However, as with other carbon-based materials, concerns have been raised over the retention of tritium and deuterium, as well as chemical etching from exposure to these species [1].

Diamond and boron doped diamond have been shown to have great potential as a PFM—demonstrating good thermal shock resistance and minimal structural changes [4–9]. More research is required to understand the interaction between CVD diamond and hydrogenic species in fusion relevant conditions in order to assess fuel retention, carbon etching and the general suitability of diamond going forward.

2. Method

2.1. Experimental

Six thermal grade, TM100, polycrystalline (PC) CVD diamond samples (provided by Element 6) were exposed to a deuterium plasma in the Device for Exposure to Low-energy Plasma of Hydrogen Isotopes (DELPHI) [10] facility at the Culham Centre for Fusion Energy (CCFE). All samples were implanted at room temperature for approximately five hours, resulting in an estimated total fluence of at least 5.5×10^{21} D m^{-2}. During implantation of each sample, deuterium ions were accelerated across potential differences of either 0.2 kV, 0.3 kV, 0.4 kV, 0.6 kV, 0.8 kV or 1 kV.

Samples were stored under vacuum for a week before analysis with Thermal Desorption Spectroscopy (TDS) using a Hiden Analytica Ltd

* Corresponding author.
E-mail address: jp17358@bristol.ac.uk (J.A. Pittard).

https://doi.org/10.1016/j.fusengdes.2022.113403
Received 14 October 2022; Received in revised form 6 December 2022; Accepted 20 December 2022
Available online 2 January 2023

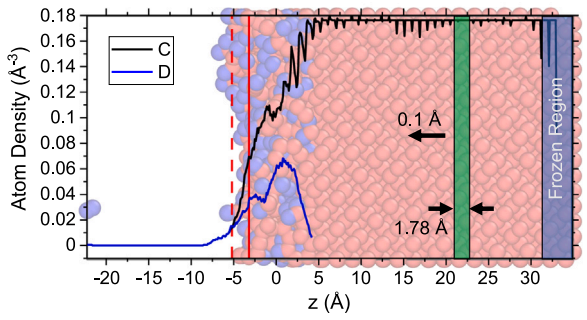

Fig. 1. Output file from partway through a LAMMPS simulation of diamond (red atoms) bombarded with deuterium atoms (blue atoms) rendered in OVITO [15], with atom density with respect to the z axis overlaid on top. At this point in the simulation, the diamond has been bombarded with 480 out of a total 4000 deuterium atoms. Atom densities were calculated by counting atoms within a half unit cell thick slice taken in z (green shaded region) every 0.1 Å through the simulation system. Atoms in a unit cell thick slice of the non-bombarded surface were frozen in place (blue shaded region). Atom densities of carbon (black) and deuterium (blue) are presented. The surface was taken to be the solid red line and the dashed line was used as an ion cut-off, beyond which ions where not considered to be implanted.

Type 640100 TPD workstation [11]. Samples were placed on a hot plate which was heated from room temperature to 1273 K, at which it was held for an hour. A heating rate of 10 K min^{-1} was used. The presence of residue from an adhesive mounting disc meant one sample required a protective aluminium nitride layer to protect the TDS from contamination. This protective layer reduced the temperature reached by the sample (resulting in lower total counts) and meant a temperature correction was required [12]. Signals of masses 2, 3 and 4 (corresponding to H_2, HD and D_2 molecules) were detected and quantified using H_2 and D_2 calibrated leaks (with the calibration factor for HD being an average between the two). In addition to the six implanted samples, another TM100 sample from Element 6 was used as a reference sample, undergoing TDS without any previous plasma exposure.

2.2. Modelling

Molecular dynamics (MD) simulations were performed in LAMMPS (Large-scale Atomic/Molecular Massively Parallel Simulator [13,14]) to complement and develop understanding of experimental results. Generally, simulations consisted of a block of diamond bombarded from below by deuterium atoms. The diamond had a (100) surface of 8 × 8 unit cells (UCs), and a depth ranging from 6–18 UCs depending on deuterium energy. Periodic boundary conditions in x and y were used, whereas non-periodic boundary conditions were selected for z. The top layer of UCs (the opposite to the bombardment side, see Fig. 1) were frozen in position to prevent any movement of the system. The frozen layer in combination with periodic boundary conditions helped to mimic a much larger system.

A variable time step was used to ensure accuracy was maintained across the range of energies tested. A default time step of 0.1 fs was used and, if required, was reduced to maintain a maximum atom movement of 0.1 Å. Simulations were performed in a NVT ensemble at a temperature of 300 K, in agreement with experimental implantation conditions. A short temperature damping parameter of 100 fs was used in order to allow the system to return to target temperature after each bombardment. The centre of mass of the frozen layer was fixed to prevent movement of the diamond during bombardment.

Deuterium atoms were created at random positions within a box 25 Å below the diamond and given positive z velocity corresponding to the desired implantation energy. Any etched atoms within this box were deleted prior to creation of the next deuterium atom. The REBO potential [16,17] was used to describe carbon–deuterium and carbon–carbon interaction. 4000 deuterium atoms where incident on the simulated diamond surfaces, with 0.5 ps between each bombardment corresponding to a fluence of 4.91 × 10^{20} D m^{-2} and a flux of 2.46 × 10^{29} D m^{-2} s^{-1}. Due to limitations of computational modelling, this flux is far higher than seen in DELPHI or in reactors [18]. However, testing showed no significant changes were observed from decreasing flux by a factor of four (for fixed fluence). Lower fluxes than this would be counterproductive, as this would limit the fluence that would be possible to simulate, and fluence has proven to be far more influential than flux. Although, the higher flux can become a concern when sputtered atoms do not have time to leave the simulation box, potentially resulting in obstruction of the next bombarding atom. This effect can be minimised by deleting etched atoms within the creation box before the next deuterium atom is created.

Simulations explored the 10–140 eV energy range. The lower end of this range represents typical energies expected to be experienced by PFMs in ITER [18], whilst the top end is closer to the hundreds of eV used in DELPHI. It proved challenging to simulate higher energies that directly overlap with experimental work. Higher energies would require much larger system sizes and increased relaxation time between bombardments to cope with the greater penetration and larger temperature fluctuations. Additionally, the increased atom velocities would require shorter time steps and, perhaps, use of a more computationally heavy potential.

Simulations were used to compare single crystal (SC) and PC diamond materials. A grain boundary was created by rotating, trimming and placing a diamond block next to another diamond block of the same size and original orientation. An energy minimisation was performed on this new data file and the resultant material was used as the initial data file for bombardment runs. Rotations of 15°, 30° and 45° with (100) surface orientation were tested.

Various methods were used to analyse simulations. Carbon and deuterium atoms were counted to calculate sputtering yields and deuterium retention. In order to do this, a surface must be determined so atoms can be classed as within the diamond or not. It was observed that the system would swell upon deuterium implantation, making surface determination challenging and the use of a fixed surface height inappropriate. Instead, the atom density of carbon with respect to z was considered. Atom density plots were made by taking a slice in z, half a UC in thickness (see Fig. 1), counting the atoms within this slice and then dividing by the slice volume. The slice began in the frozen region, then the z limits of the slice moved 0.1 Å along the simulation box and the atoms were recounted. This process was repeated until the length of the simulation box had been considered, and an atom density value for each z value had been calculated. The surface height was taken to be the first z value that the atom density values of the previous 2 Å averaged below half the density of pristine diamond. Carbon outside of the surface line was considered to be etched, whilst monitoring of surface height as the simulation progressed gave an insight into swelling and etching of the diamond. To allow for surface bonding, a secondary line 2 Å from the surface was considered as the cut-off for deuterium. Any deuterium beyond this cutoff would not be considered as implanted. Atom density against z for deuterium atoms was also determined to give depth profiles.

3. Results and discussion

3.1. Experimental

Fig. 2 presents a comparison of TDS spectra for the six samples implanted at different energies and the reference sample which was not implanted. It can be seen in Fig. 2a that, as the implantation energy of deuterium ions increased, an additional release peak in the 900–1100 K temperature range appears. A peak in this temperature range was not observed in HD or H_2 spectra (Fig. 2b and Fig. 2c

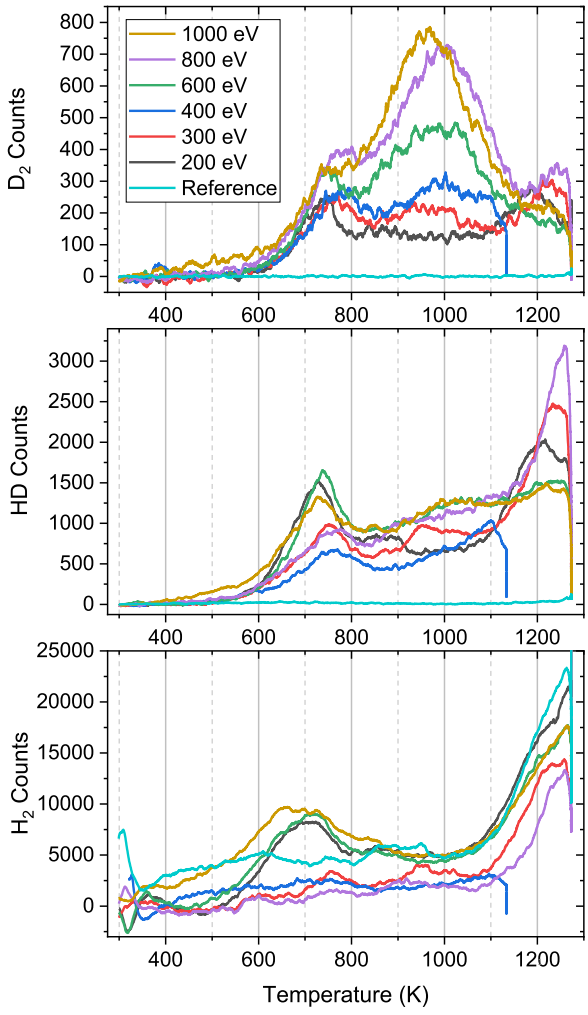

Fig. 2. (a, b and c) TDS spectra of masses 4 (D_2), 3 (HD) and 2 (H_2) respectively, taken from six polycrystalline CVD diamond samples provided by Element 6 post deuterium implantation at various energies and one reference sample without implantation. Samples were heated at a ramp rate of 10 K min^{-1} from room temperature to 1273 K at which it was held for an hour. The 400 eV sample (blue) required a protective aluminium nitride layer, resulting in a reduced maximum temperature and the need for a temperature correction.

respectively) and differences between sample spectra appears to have minimal dependence on implantation energy for these masses.

Hydrogen and deuterium were incorporated into the diamond in different manners; the former was incorporated from the gas phase during growth, whilst the latter was energetically implanted. Differences in H_2 and D_2 spectra are likely to be a result of these differing processes. CVD diamond growth is conducted in a high hydrogen environment, as hydrogen preferentially etches sp^2C-C over sp^3C-C, so such an environment promotes the growth of diamond rather than graphitic phases [19]. As a consequence of this, CVD diamond typically displays a high hydrogen content with the majority residing within grain boundaries [20]. Therefore, peaks seen in H_2 spectra are likely to correspond to grain boundary binding sites. In contrast, deuterium was energetically implanted, meaning a wider variety of binding sites were available compared to the low energy hydrogen. Due to the similar mass and bonding mechanisms of hydrogen and deuterium, it would be expected that equivalent binding sites would desorb at the same temperature. As such, the first peak seen in the 600–800 K temperature range which is seen in some of the H_2, HD and D_2 spectra is attributed to deuterium coming from grain boundary binding sites, as is the third peak seen above 1100 K. The second peak seen in the D_2 spectra (in the 800–1100 K range) becomes more prominent with increasing implantation energy. No significant peak in this temperature range can be seen in H_2 or HD spectra, suggesting the binding sites associated with this peak was not accessible to hydrogen bound within the diamond. Inter-grain binding sites therefore seem a likely candidate for this temperature range, as minimal hydrogen would be found within grains. It is also logical that increasing the implantation energy would result in a greater amount of deuterium successfully penetrating the grains.

As the initial peak (600–800 K) is present in spectra of all masses (if not all samples) it is likely that desorption in this range is associated with weakly bound hydrogen/deuterium within grain boundaries. Simultaneous hydrogen and deuterium desorption is further supported by the presence of a peak in HD spectra. No trends can be seen between implantation energy and the presence of a H_2 peak in this region with 300, 400 and 800 eV samples not presenting H_2 peak in this temperature range. The absence of this peak in these samples is likely due to variation in growth conditions, as these samples were acquired together it is probable they were grown in the same batch. Similarly, the 200, 600 and 1000 eV samples were also acquired as a set and all presented a peak in the 600–800 K range.

Differences between the initial (600–800 K) and central (800–1100 K) peaks are a result of hydrogen/deuterium location rather than differences in bonding type. Another experiment, with a similar setup, also observed a deuterium TDS peak in the 700–1100 K range for a diamond exposed to 1000 eV deuterium ions [21]. In agreement with the interpretation of grain desorption presented here, these deuterium counts were attributed to sp^3C-D defects. Hydrogen and deuterium are expected to form sp^3C-H and sp^3C-D defects respectively, upon interaction with both sp^3C-C and sp^2C-C [21]. As a result of this, despite grain boundaries having a higher sp^2C-C content [5], there is overlap between these two peaks in D_2 counts. The absence of release peaks in the 800–1100 K range in HD and H_2 spectra shows a clear distinction between this and the 600–800 K region. Hence, the presence of the central peak is dictated by location not bonding type.

As the high temperature peak at > 1100 K is prominent in HD and H_2 spectra, it is likely to correspond to grain boundary desorption. Some D_2 spectra also displayed a high temperature peak and, as with the initial peak, this was also interpreted as grain boundary desorption due to the presence of HD and H_2 peaks in this region. Significant hydrogen diffusion would be expected at these higher temperatures [22], allowing hydrogen/deuterium from deeper within the crystal outgas. The prominence of H_2 and HD compared to D_2 suggests some desorption of hydrogen beyond the interaction volume of the deuterium and the possibility of hydrogen collecting deuterium whilst diffusing to the surface. This explanation is further supported by Fig. 3, which shows hydrogen counts from TDS against time, presenting hydrogen desorption during the hour fixed at 1273 K (from approximately 5800 s onwards). Once held at 1273 K, H_2 desorption of deuterium implanted samples settles at a flat rate. This constant outgassing of H_2 would be expected for hydrogen diffusing out of the diamond, instead of a peak in desorption which would suggest a particular binding type that requires some threshold energy to desorb. The 400 eV sample was disregarded from this figure as the temperature correction made comparing desorption with respect to time against other samples invalid. Currently, it is unclear why the reference sample does not display the flat desorption rate of the deuterium implanted samples. The deuterium desorption in this fixed temperature region is predominately HD, as the amount of deuterium to successful penetrate to these deeper depths is minimal and a greater amount of hydrogen relative to deuterium is present. Furthermore, the 800 eV sample showed the lowest H_2 counts with the highest D_2 counts at this peak, suggesting presence of hydrogen could be limiting deuterium uptake deeper within grain boundaries. Deuterium peaks at this temperature range in similar set ups have been attributed to D_2 bubbles produced during implantation [21]. This

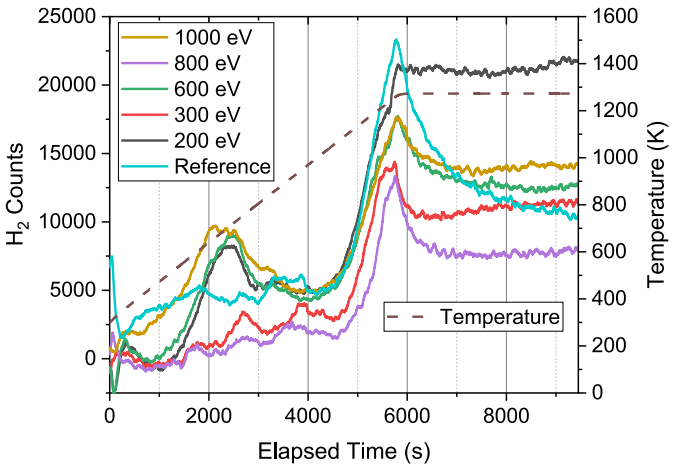

Fig. 3. TDS spectra of mass 2, attributed to H_2 counts, for five polycrystalline CVD diamond samples provided by Element 6 post deuterium implantation at various energies. Samples were heated at a ramp rate of 10 K min^{-1} from room temperature to 1273 K at which it was held for an hour. A typical temperature profile (brown dashed line) is also included. Hydrogen is incorporated into the diamond during growth rather then energetic implantation.

Table 1
Calibrated total counts from TDS data of six polycrystalline diamond samples implanted with deuterium at various energies.

TDS total counts			
Implantation energy	HD $\times 10^{15} cm^{-2}$	D_2 $\times 10^{15} cm^{-2}$	Total D $\times 10^{15} cm^{-2}$
200 eV	3.62	0.925	5.47
300 eV	2.99	0.579	4.15
400 eV	1.72*	0.652*	3.02*
600 eV	3.21	0.933	5.08
800 eV	3.67	1.19	6.05
1000 eV	3.18	1.25	5.67
Reference	0.249	0.041	0.331

Note values marked * were heated to a lower max temperature, giving lower total count values.

explanation seems unlikely from the results presented here, as this peak is most prominent for the grown-in hydrogen of the reference sample.

As can be seen in Table 1, there is reasonable variation in total count values from the TDS. Conclusions drawn between total counts alone are limited. These differences are likely to be a result of disparities in implantation fluence and between the samples themselves rather than solely correlated with implantation energy. No trends between total HD counts and implantation energy can be seen but the highest energies resulted in the highest D_2 counts. These observations support the inter-grain penetration theory, as deuterium and hydrogen desorption at the same temperature is likely to be from equivalent binding sites—with the presence of hydrogen suggesting grain boundary desorption. As such, peaks in HD correspond to easily accessible grain boundary desorption and would be expected to be largely uncorrelated with implantation energy. Whereas the amount of D_2 implanted in grains would increase with energy. Furthermore, it can be said that these values are comparable to values of metal PFM candidates tested in the same experimental set up [10,23,24]. It is worth noting the peak seen in the > 1100 K range in Fig. 2 is at higher temperatures than peaks observed in these studies. Therefore, it is plausible that more deuterium remains within diamond samples post TDS than in the metal samples, which could contribute to comparably lower counts in diamond samples.

Deslandes et al. [25] obtained approximately three times the deuterium retention for equivalent samples from Element 6. Samples were exposed to a deuterium plasma with an electron temperature of 5 eV, resulting in an estimated incident ion energy of 18 eV and a comparable fluence. The flux used was four orders of magnitude higher than DELPHI, and would be expected effect retention. Despite the lower energy, the higher flux could cause greater disruption in the crystal, create more binding sites and increase retention. The different ion energies makes the results hard to directly compare. Higher energies will have a greater interaction volume within the crystal, leading to higher retention from the increased number of available binding sites. However, higher energies also result in greater etching of both carbon and deuterium, potentially lowering the total retention. Both experimental and computational work presented here showed retention increasing with energy, suggesting the former argument is dominating. Retention values could also be impacted on the analysis method, Deslandes et al. used elastic recoil detection analysis (ERDA) which infers the presence of deuterium through recoil energies rather than direct measurement with a mass spectrometer. Sample temperature is not specified and could also have an impact.

3.2. Modelling

Results from MD simulations suggest a two-step etching mechanism. Initially, incident deuterium atoms are unable to sputter carbon atoms in the energy range studied here, but are able to penetrate small distances (of order nm) into the surface. With increasing fluence, more deuterium atoms penetrate the diamond, resulting in a disordered region and swelling as the diamond loses its close packed structure. Eventually a point is reached where the disordered carbon atoms etch away from the surface.

The swelling and etching phases can be seen in Fig. 4, which shows the surface height as the simulation progresses alongside atom density plots from key points of the simulations. Negative surface height values show the swelling of the surface before the etch point is reached. Density plots at this point (the two central plots) shows an expanded sub surface region of lower density. In the etching phase, the higher energy implantation results in carbon being removed in clusters as seen in the steps in surface height for 100 eV implantation. The lower energy displays a much more controlled, steady and consistent etching phase due to the smaller disordered region, giving less opportunity for large clumps of carbon to be removed. A shorter swelling phase and slower etching is observed for lower energies (see Fig. 5).

Fig. 6 shows sputtering yields calculated using two methods. The final count method is calculated in the standard manner, where sputtering yield, S_{count}, is given by taking the ratio of etched carbon, N_C over incident deuterium, N_D.

$$S_{count} = \frac{N_C}{N_D}. \quad (1)$$

Whereas, the volume removed method used the volume etched per deuterium atom, V_{etch}, for various energies once the etching phase had been reached. V_{etch} values were found by taking linear fits of surface height (on equivalent plots to those seen in Fig. 5) after the etch point had been reached. Once the etch point is reached, a roughly linear etch rate would be expected from the regular atom bombardments. The average volume occupied by a single carbon atom was taken to be an $\frac{1}{8}$ of a UC's volume, allowing V_{etch} to be converted to a sputtering yield, S_{vol}, via

$$S_{vol} = \frac{8V_{etch}}{(3.567\ \text{Å})^3}. \quad (2)$$

Values calculated in this manner are approximately equivalent to values calculated via the final count method, but the volume removed method allows an average over the etching phase to be taken. S is approximately linear with energy for both methods, with the volume removed method giving a gradient of $0.0083 \pm 0.0005\ eV^{-1}$. This linear dependence is typical of the knock-on sputtering regime [26], where incident ions are of greater energy than the surface binding energy and are able to dislodge bound particles. As this point is only reached after

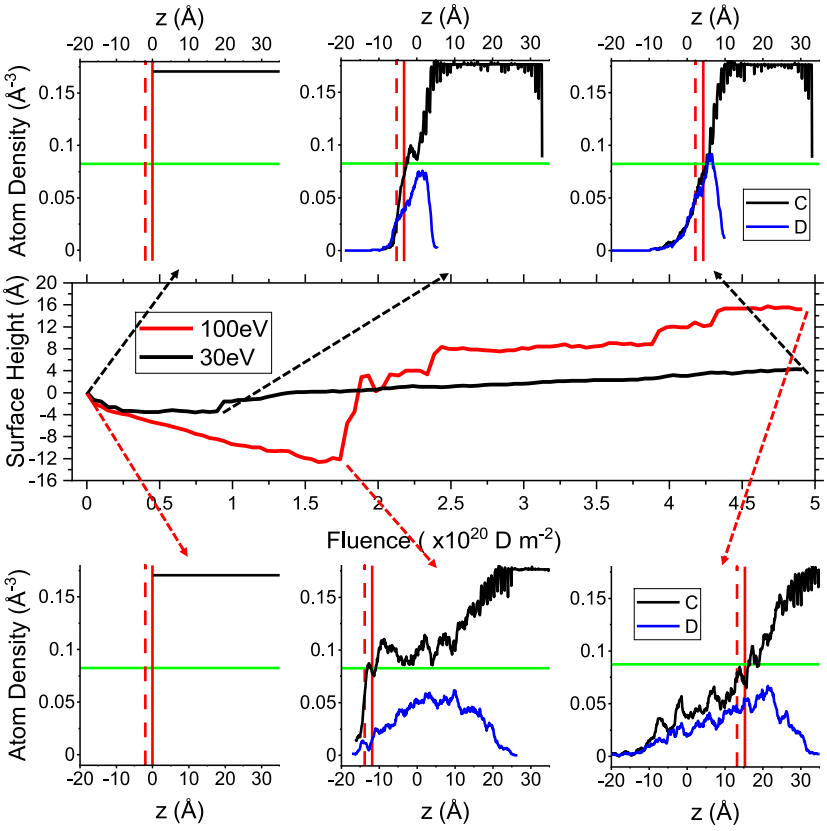

Fig. 4. Results from LAMMPS simulations of 30 eV and 100 eV deuterium bombardments on diamond. Central figure shows the surface heights of the diamond as the simulations progress. The six surrounding plots show atom density of carbon and deuterium atoms against the z axis at three points in the simulations. The two central density plots show the etch point—where the maximum swelling of the surface has occurred, and etching is about to begin. The definition of the surface (solid red vertical line) was based on the point where carbon atom density dropped below 50% (solid green line) of pristine diamond. Dashed red line shows the ion cut-off, beyond which, ions were not considered to be implanted.

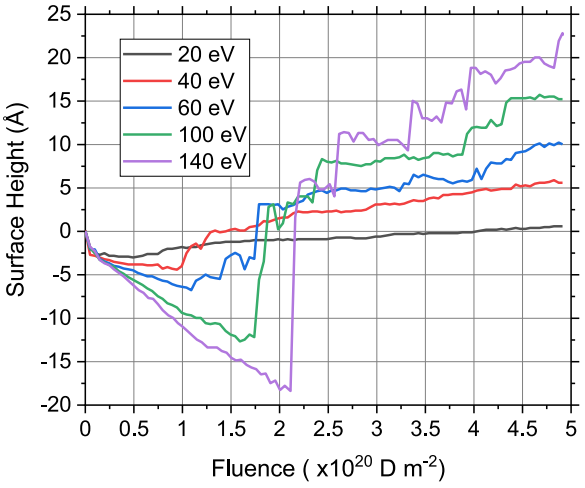

Fig. 5. Surface height of single crystal diamond bombarded with 4000 deuterium atoms at set energies simulated in LAMMPS. The determination of the surface was based off of the point where the atom density with respect to the z axis dropped below 50% of pristine diamond. Negative values show swelling of the surface from the initial height (0 Å) whereas positive gradients show etching.

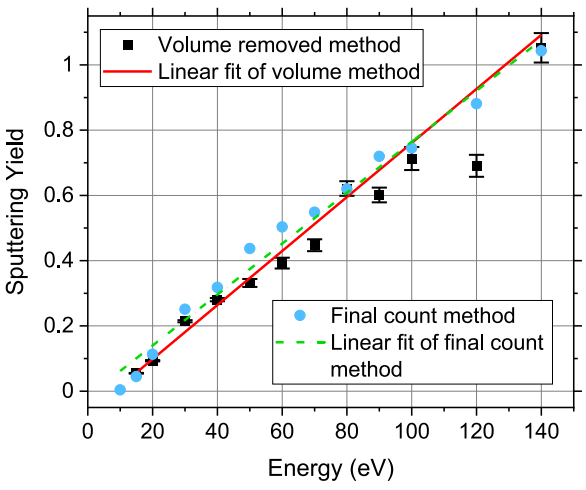

Fig. 6. Sputtering yield calculated by two methods from LAMMPS simulations of single crystal diamond bombarded with deuterium atoms at a set energy. The volume etched method was calculated by taking a linear fit of surface height with respect to fluence once the etching phase had begun and assuming an atom occupies an average volume of $\frac{1}{8}$ of a unit cell. Errors were taken to be the error on the linear fit. The final point method took the ratio of implanted to incident deuterium atoms. Linear fit of volume removed method: Gradient = 0.0083 ± 0.0005 eV^{-1}, y-intercept = -0.07 ± 0.01. Linear fit of final count method: 0.0078 ± 0.0003, y-intercept = -0.02 ± 0.02.

the swelling, this would suggest a decrease in binding energy in the post swelling disordered carbon region as would be expected. In the 10 eV simulation, the volume method could not be applied as a clear etching phase could not be seen.

With increasing deuterium energy, more deuterium is retained, with the peak of the depth profile located deeper within the material

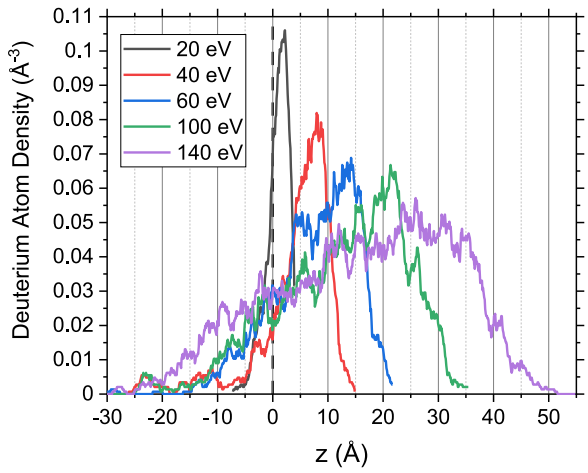

Fig. 7. Deuterium depth profiles from five LAMMPS simulations of single crystal diamond bombarded with deuterium atoms at a set energy. The (100) diamond surface had a 8 × 8 unit cell surface area and was bombarded with 4000 D atoms, giving a total fluence of 4.91 × 10^{20} D m^{-2}. The original diamond surface was at 0 Å.

as seen in Fig. 7. Generally, penetration depths were low, with the highest energy, 140 eV, showing a peak in the depth profile around 2.5 nm from the initial surface and max penetration of around 5 nm. The diamond below the interaction volume remained pristine post implantation. The broader deuterium profiles observed for higher energy implantation also resulted in more deuterium located at negative z values (outside the initial material). This is a consequence of the larger disordered region allowing trapping of deuterium a greater distance from the initial surface, which can be seen in the final density plots in Fig. 4. Total retention for simulations and experimental work were to the same order (10^{15} D m^{-2}). As previously discussed, Deslandes et al. [25], experimentally obtained a higher retention value for an ion energy more comparable to the computational work presented here. Therefore, it might be expected that the simulations may give higher retention values than those obtained. However, factors such as the perfect crystalline structure and perfectly flat surface (reducing surface area) would all go towards reducing deuterium retention for a set energy.

For simulations of systems containing a grain boundary, no discernible differences between retention or etching could be seen when compared to the SC system across the energies tested. Despite this result, the presence of grain boundaries at the higher energies used in DELPHI could still have an effect. At such energies, incident deuterium atoms may be able to remove carbon atoms without the swelling seen in computational work. There are other differences between computational and experimental work, such as the presence of hydrogen in the crystal which would be expected to reduce deuterium retention but increase disorder in the structure. Additionally, clusters of deuterium (with an average size of 2.98 D atoms [10]) were incident in DELPHI, compared to the single deuterium atoms that were simulated. This larger mass would be expected to reduce penetration depth for the same energy, which can be shown by considering a head on collision. For the incident particle of mass m, directly colliding with a stationary particle of mass M, the ratio of final kinetic energy, ϵ_f, to initial kinetic energy, ϵ_i, for the incoming particle is given by

$$\frac{\epsilon_f}{\epsilon_i} = \left(\frac{m-M}{m+M}\right)^2. \quad (3)$$

Hence, going from the simulated mass of 2 u, to the average experimental mass of 5.96 u, would give a drop in the energy carried through the collision from 51% to 11%. A larger degree of energy would also be transferred to the stationary carbon atom. Therefore, the larger mass would be expected to reduce penetration depths but increase damage, and would have a significant impact on etching and retention. The smaller interaction volume might have behaved similarly to the lower energy implantations, with reduced swelling and a more consistent etching rate.

Similar computational models were conducted by Dunn et al. [27], in which a variety of diamond surface orientations where bombarded with 15 eV tritium atoms. Comparing these results to results obtained for the 15 eV deuterium implantation presented here, shows very similar retention values (approx. 4.5×10^{19} T m^{-2} compared to 4.3×10^{19} D m^{-2}). The etch rate of 0.073 obtained by Dunn et al. deviated slightly from S_{vol} and S_{count} values of 0.055 and 0.045 respectively. This could be a result of the larger mass of tritium compared to deuterium. As seen in Eq. (3), for a fixed ϵ_i, a larger mass would result in greater energy transfer to the stationary particle, increasing the likelihood of sputtering. For an equal ϵ_f, the initial energy of a deuterium would need to be around 19.6 eV, or for an equal final momentum, 22.5 eV. This small increase in energy would result in a slightly higher sputtering yield as seen in Fig. 6. Other differences between simulations are also likely to play a role, such as the lower flux used in this study and subtle differences in temperature scaling. Although not discussed by Dunn et al. in depth, an initial period of reduced etching can also be seen in the results presented, similar to the two-step etching mechanism described here.

4. Conclusion

Deuterium implantation of PC diamond films was used to study the interaction between deuterium plasma and diamond. Through comparison of hydrogen and deuterium spectra, peaks in different temperature regions of TDS spectra were attributed to differing deuterium locations, rather than bonding types. Peaks seen in both hydrogen and deuterium spectra were attributed to grain boundary desorption, and were observed at low temperatures (600–800 K) as well as high temperatures (> 1100 K). It is believed the latter peak is a result of hydrogen diffusion through grain boundaries once a sufficient temperature was reached. A peak was observed between 800–1100 K in D_2 spectra for samples implanted at high energies which was assigned to deuterium from within the grains.

LAMMPS simulations were performed at lower energies (more typical of fusion reactors) and demonstrated a two-step etching mechanism of swelling to a disordered structure prior to carbon removal. In these simulations, in the energy range tested, no significant differences could be seen between SC systems, and systems containing a grain boundary. The comparisons that can be made between experimental work and simulations are reduced due to the different energy regimes, deuterium cluster size and diamond hydrogen content.

Total retention for simulations and experimental work was to the same order and both were comparable, or lower, than retention values of other PFM candidates tested in the same experimental set up [10,23,24], suggesting good potential for diamond as a PFM.

Use of SC materials could have a significant benefit in the 100–400 eV energy range when it is believed the majority of deuterium uptake is from binding sites within grain boundaries. However, at energies more relevant for fusion reactors explored with simulations, no significant differences in etch rate or retention could be seen on the inclusion of a grain boundary, suggesting limited benefit of SC diamond over PC diamond.

Declaration of competing interest

The authors declare that they have no known competing financial interests or personal relationships that could have appeared to influence the work reported in this paper.

Data availability

Data will be made available on request.

Acknowledgements

The first author acknowledges the support of Engineering and Physical Sciences Research Council, United Kingdom, and UKAEA, United Kingdom. This work was carried out using the computational facilities of the Advanced Computing Research Centre, University of Bristol - http://www.bris.ac.uk/acrc. We would also like to thank Prof. Neil L. Allan of the University of Bristol for his useful comments on computational work.

References

[1] D. Duffy, Modeling plasma facing materials for fusion power, Mater. Today 12 (11) (2009) 38–44, http://dx.doi.org/10.1016/S1369-7021(09)70297-4, URL https://www.sciencedirect.com/science/article/pii/S1369702109702974.

[2] B. Kalin, A. Suchkov, V. Fedotov, O. Sevryukov, A. Ivannikov, A. Gervash, Brazing of Be with CuCrZr-bronze using copper-based filler metal STEMET, Nucl. Mater. Energy 9 (2016) 388–393, http://dx.doi.org/10.1016/j.nme.2016.07.004, URL https://www.sciencedirect.com/science/article/pii/S2352179115300636.

[3] T. Hirai, S. Panayotis, V. Barabash, C. Amzallag, F. Escourbiac, A. Durocher, M. Merola, J. Linke, T. Loewenhoff, G. Pintsuk, M. Wirtz, I. Uytdenhouwen, Use of tungsten material for the ITER divertor, Nucl. Mater. Energy 9 (2016) 616–622, http://dx.doi.org/10.1016/j.nme.2016.07.003, URL https://www.sciencedirect.com/science/article/pii/S2352179115301046.

[4] G.D. Temmerman, J. Dodson, J. Linke, S. Lisgo, G. Pintsuk, S. Porro, G. Scarsbrook, Thermal shock resistance of thick boron-doped diamond under extreme heat loads, Nucl. Fusion 51 (5) (2011) 052001, http://dx.doi.org/10.1088/0029-5515/51/5/052001.

[5] S. Porro, G. De Temmerman, P. John, S. Lisgo, I. Villalpando, J.I.B. Wilson, Effects in CVD diamond exposed to fusion plasmas, Phys. Status Solidi (A) 206 (9) (2009) 2028–2032, http://dx.doi.org/10.1002/pssa.200982201, URL https://onlinelibrary.wiley.com/doi/abs/10.1002/pssa.200982201.

[6] S. Porro, G.D. Temmerman, S. Lisgo, D. Rudakov, A. Litnovsky, P. Petersson, P. John, J. Wilson, Diamond coatings exposure to fusion-relevant plasma conditions, J. Nucl. Mater. 415 (1, Supplement) (2011) S161–S164, http://dx.doi.org/10.1016/j.jnucmat.2010.10.005, Proceedings of the 19th International Conference on Plasma-Surface Interactions in Controlled Fusion. URL https://www.sciencedirect.com/science/article/pii/S0022311510005714.

[7] S. Porro, G. De Temmerman, D. MacLaren, S. Lisgo, D. Rudakov, J. Westerhout, M. Wiora, P. John, I. Villalpando, J. Wilson, Surface analysis of CVD diamond exposed to fusion plasma, Diam. Relat. Mater. 19 (7) (2010) 818–823, http://dx.doi.org/10.1016/j.diamond.2010.01.051, Proceedings of Diamond 2009, The 20th European Conference on Diamond, Diamond-Like Materials, Carbon Nanotubes and Nitrides, Part 2. URL https://www.sciencedirect.com/science/article/pii/S0925963510000713.

[8] S. Porro, G. De Temmerman, S. Lisgo, P. John, I. Villalpando, J.W. Zimmer, B. Johnson, J.I. Wilson, Nanocrystalline diamond coating of fusion plasma facing components, Diam. Relat. Mater. 18 (5) (2009) 740–744, http://dx.doi.org/10.1016/j.diamond.2009.01.006, Proceedings of Diamond 2008, the 19th European Conference on Diamond, Diamond-Like Materials, Carbon Nanotubes, Nitrides and Silicon Carbide. URL https://www.sciencedirect.com/science/article/pii/S0925963509000065.

[9] G.D. Temmerman, R.P. Doerner, P. John, S. Lisgo, A. Litnovsky, L. Marot, S. Porro, P. Petersson, M. Rubel, D.L. Rudakov, G.V. Rooij, J. Westerhout, J.I.B. Wilson, Interactions of diamond surfaces with fusion relevant plasmas, Phys. Scr. T138 (2009) 014013, http://dx.doi.org/10.1088/0031-8949/2009/t138/014013.

[10] A. Hollingsworth, M.Y. Lavrentiev, R. Watkins, A.C. Davies, S. Davies, R. Smith, D. Mason, A. Baron-Wiechec, Z. Kollo, J. Hess, I. Jepu, J. Likonen, K. Heinola, K. Mizohata, E. Meslin, M.-F. Barthe, A. Widdowson, I.S. Grech, K. Abraham, E. Pender, A. McShee, Y. Martynova, M. Freisinger, A.D. Backer, Comparative study of deuterium retention in irradiated eurofer and Fe–Cr from a new ion implantation materials facility, Nucl. Fusion 60 (1) (2019) 016024, http://dx.doi.org/10.1088/1741-4326/ab546e.

[11] A. Baron-Wiechec, K. Heinola, J. Likonen, E. Alves, N. Catarino, J. Coad, V. Corregidor, I. Jepu, G. Matthews, A. Widdowson, Thermal desorption spectrometry of beryllium plasma facing tiles exposed in the JET tokamak, Fusion Eng. Des. 133 (2018) 135–141, http://dx.doi.org/10.1016/j.fusengdes.2018.05.075, URL https://www.sciencedirect.com/science/article/pii/S0920379618305088.

[12] Y. Zayachuk, et al., Fuel desorption from JET-ILW materials: Assessment of analytical approach and identification of uncertainty and discrepancy sources, in Preparation.

[13] P.J. in 't Veld, S.J. Plimpton, G.S. Grest, Accurate and efficient methods for modeling colloidal mixtures in an explicit solvent using molecular dynamics, Comput. Phys. Comm. 179 (5) (2008) 320–329, http://dx.doi.org/10.1016/j.cpc.2008.03.005, URL https://www.sciencedirect.com/science/article/pii/S001046550800115X.

[14] A.P. Thompson, H.M. Aktulga, R. Berger, D.S. Bolintineanu, W.M. Brown, P.S. Crozier, P.J. in 't Veld, A. Kohlmeyer, S.G. Moore, T.D. Nguyen, R. Shan, M.J. Stevens, J. Tranchida, C. Trott, S.J. Plimpton, LAMMPS - a flexible simulation tool for particle-based materials modeling at the atomic, meso, and continuum scales, Comput. Phys. Comm. 271 (2022) 108171, http://dx.doi.org/10.1016/j.cpc.2021.108171, URL https://www.sciencedirect.com/science/article/pii/S0010465521002836.

[15] A. Stukowski, Visualization and analysis of atomistic simulation data with OVITO–the open visualization tool, Modelling Simul. Mater. Sci. Eng. 18 (1) (2009) 015012, http://dx.doi.org/10.1088/0965-0393/18/1/015012.

[16] D.W. Brenner, O.A. Shenderova, J.A. Harrison, S.J. Stuart, B. Ni, S.B. Sinnott, A second-generation reactive empirical bond order (REBO) potential energy expression for hydrocarbons, J. Phys.: Condens. Matter 14 (4) (2002) 783–802, http://dx.doi.org/10.1088/0953-8984/14/4/312.

[17] D.W. Brenner, Empirical potential for hydrocarbons for use in simulating the chemical vapor deposition of diamond films, Phys. Rev. B 42 (1990) 9458–9471, http://dx.doi.org/10.1103/PhysRevB.42.9458, URL https://link.aps.org/doi/10.1103/PhysRevB.42.9458.

[18] G. Federici, J.N. Brooks, M. Iseli, C.H. Wu, In-vessel tritium retention and removal in ITER-FEAT, Phys. Scr. T91 (1) (2001) 76, http://dx.doi.org/10.1238/physica.topical.091a00076.

[19] M. Schwander, K. Partes, A review of diamond synthesis by CVD processes, Diam. Relat. Mater. 20 (9) (2011) 1287–1301, http://dx.doi.org/10.1016/j.diamond.2011.08.005, URL https://www.sciencedirect.com/science/article/pii/S0925963511002913.

[20] J.P. Goss, R. Jones, M.I. Heggie, C.P. Ewels, P.R. Briddon, S. Öberg, Theory of hydrogen in diamond, Phys. Rev. B 65 (2002) 115207, http://dx.doi.org/10.1103/PhysRevB.65.115207, URL https://link.aps.org/doi/10.1103/PhysRevB.65.115207.

[21] H. Kimura, M. Sasaki, Y. Morimoto, T. Takeda, H. Kodama, A. Yoshikawa, M. Oyaidzu, K. Takahashi, K. Sakamoto, T. Imai, K. Okuno, Thermal desorption behavior of deuterium implanted into polycrystalline diamond, J. Nucl. Mater. 337–339 (2005) 614–618, http://dx.doi.org/10.1016/j.jnucmat.2004.10.079, PSI-16. URL https://www.sciencedirect.com/science/article/pii/S0022311504008451.

[22] D. Ballutaud, F. Jomard, B. Theys, C. Mer, D. Tromson, P. Bergonzo, Hydrogen diffusion and stability in polycrystalline CVD undoped diamond, Diam. Relat. Mater. 10 (3) (2001) 405–410, http://dx.doi.org/10.1016/S0925-9635(00)00590-2, 11th European Conference on Diamond, Diamond-like Materials, Carbon Nanotubes, Nitrides and Silicon Carbide. URL https://www.sciencedirect.com/science/article/pii/S0925963500005902.

[23] A. Hollingsworth, M.-F. Barthe, M.Y. Lavrentiev, P. Derlet, S. Dudarev, D. Mason, Z. Hu, P. Desgardin, J. Hess, S. Davies, B. Thomas, H. Salter, E. Shelton, K. Heinola, K. Mizohata, A. De Backer, A. Baron-Wiechec, I. Jepu, Y. Zayachuk, A. Widdowson, E. Meslin, A. Morellec, Comparative study of deuterium retention and vacancy content of self-ion irradiated tungsten, J. Nucl. Mater. 558 (2022) 153373, http://dx.doi.org/10.1016/j.jnucmat.2021.153373, URL https://www.sciencedirect.com/science/article/pii/S0022311521005936.

[24] M.Y. Lavrentiev, A. Hollingsworth, J. Hess, S. Davies, A. Wohlers, B. Thomas, H. Salter, A. Baron-Wiechec, I. Jepu, Y. Zayachuk, N. Peng, Effects of self-irradiation on deuterium retention and reflectivity of molybdenum, fusion plasma-facing material: Combined experimental and modeling study, J. Appl. Phys. 132 (12) (2022) 125902, http://dx.doi.org/10.1063/5.0099051, arXiv:https://doi.org/10.1063/5.0099051.

[25] A. Deslandes, M.C. Guenette, C.S. Corr, I. Karatchevtseva, L. Thomsen, G.R. Lumpkin, D.P. Riley, Deuterium retention and near-surface modification of ion-irradiated diamond exposed to fusion-relevant plasma, Nucl. Fusion 54 (2014) http://dx.doi.org/10.1088/0029-5515/54/7/073003, URL https://iopscience.iop.org/article/10.1088/0029-5515/54/7/073003.

[26] A.H. Simon, 4 - sputter processing, in: K. Seshan (Ed.), Handbook of Thin Film Deposition (Third Edition), third ed., William Andrew Publishing, Oxford, 2012, pp. 55–88, http://dx.doi.org/10.1016/B978-1-4377-7873-1.00004-8, URL https://www.sciencedirect.com/science/article/pii/B9781437778731000048.

[27] A.R. Dunn, D.M. Duffy, A.M. Stoneham, A molecular dynamics study of diamond exposed to tritium bombardment for fusion applications, vol. 269, 2011, pp. 1724–1726, http://dx.doi.org/10.1016/j.nimb.2010.12.009, URL https://www.sciencedirect.com/science/article/pii/S0168583X10009420,